Host–Guest Systems

Cavity Effects on the Enantioselectivity of Chiral Amido[4]resorcinarene Stereoisomers**

*Bruno Botta, Deborah Subissati, Andrea Tafi, Giuliano Delle Monache, Antonello Filippi, and Maurizio Speranza**

Enzyme catalysis plays a crucial role in all biochemical processes. Natural and artificial enzymes normally exhibit a high enantioselectivity toward chiral molecules as a consequence of shape-specific noncovalent attractive and repulsive intermolecular interactions.[1–5] An important step toward the elucidation of enzyme mechanisms requires a comprehensive kinetic study using simplified models under conditions, such as the gas phase, where the molecule/receptor interactions are not perturbed by medium effects.[6]

Calixarenes lend themselves to this task since they are synthetic macrocycles endowed with a cavity-shaped architecture, which can be made asymmetric by the presence of chiral pendant groups. A peculiar feature of calixarene macrocycles is their nonplanar cyclophane structure, which may give rise to relatively stable stereoisomeric and conformational forms. A pertinent case is that of 2,8,14,20-tetrakis(L-valinamido)[4]resorcinarene (**1**), which can display at least four stable stereoisomeric structures, that is, flattened cone ($\mathbf{1a_L}$), 1,2-alternate ($\mathbf{1b_L}$), chair 1 ($\mathbf{1c_L}$) (Figure 1), and chair 2.[7] Its stereoisomerism allows the tailoring of variously shaped cavities, which can be probed to evaluate their effect on ion or molecular recognition.[8,9]

Herein, we report the first comparative gas-phase study along these lines. The intrinsic enantioselectivity of the $\mathbf{1a_L}$, $\mathbf{1b_L}$, and $\mathbf{1c_L}$ diastereomeric structures was checked by introducing their proton-bonded complexes with the pure D and L enantiomers of some aromatic amino acids (A), such as phenylalanine (Phe), tyrosine (Tyr), and 3,4-dihydroxyphenylalanine (dopa), into the cell of a Fourier-transform ion cyclotron resonance mass spectrometer (FT-ICR-MS) and measuring the exchange rate of the amino acid A with

[*] Prof. B. Botta, Dr. D. Subissati, Dr. A. Filippi, Prof. M. Speranza
Dipartimento di Studi di Chimica e Tecnologia
delle Sostanze Biologicamente Attive
Università "La Sapienza", 00185 Roma (Italy)
Fax: (+39) 06-4991-3602
E-mail: maurizio.speranza@uniroma1.it
Prof. A. Tafi
Dipartimento Farmaco Chimico Tecnologico
Università di Siena, 53100 Siena (Italy)
Dr. G. Delle Monache
Istituto Chimica del Riconoscimento Molecolare
Università Cattolica del Sacro Cuore, 00168 Roma (Italy)

[**] This work was supported by the Ministero dell'Istruzione dell'Università e della Ricerca (MIUR) and the Consiglio Nazionale delle Ricerche (CNR). The authors express their gratitude to F. Angelelli for technical assistance.

Supporting information for this article is available on the WWW under http://www.angewandte.org or from the author.

 DOI: 10.1002/anie.200460663

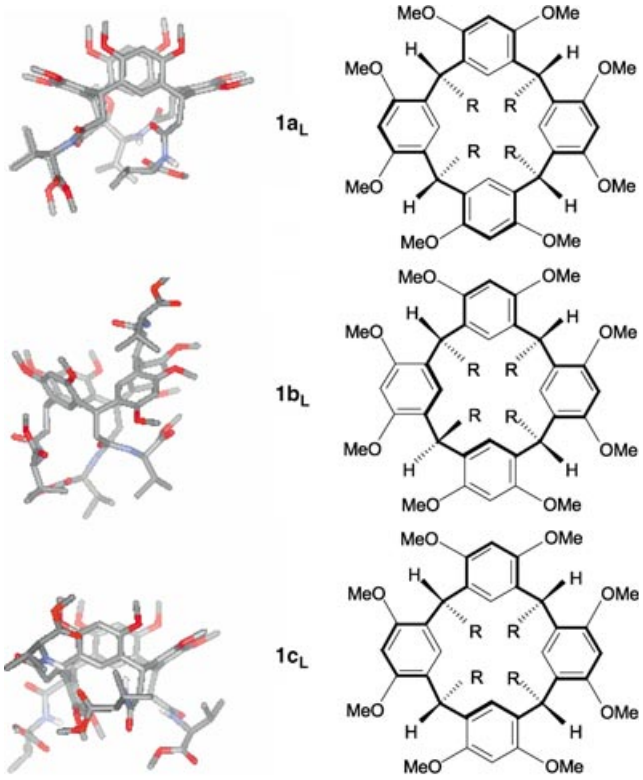

Figure 1. Formulas and side views of local minimum geometry of 2,8,14,20-tetrakis(L-valinamido)[4]resorcinarene (R = L-CH_2CONH-CH(*i*Pr)COOEt) in the flattened-cone **1a**$_L$, 1,2-alternate **1b**$_L$, and chair 1 **1c**$_L$ structures.

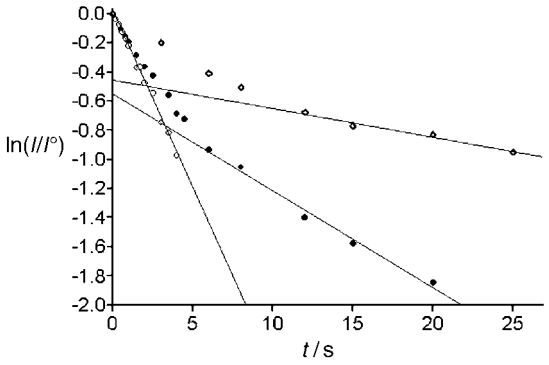

Figure 2. Kinetic plots for the gas-phase reaction between (*R*)-(−)-2-butylamine (B_R) and $[(\mathbf{1c_L})\cdot H\cdot A]^+$ (A = L-Phe (open circles; $P(B_R) = 4.1\times10^{-8}$ mbar); L-Tyr (solid circles; $P(B_R) = 6.2\times10^{-8}$ mbar); L-dopa (diamonds; $P(B_R) = 2.6\times10^{-7}$ mbar)).

(*S*)-(+)- and (*R*)-(−)-2-butylamine (B_S and B_R, respectively) [Eq. (1)].

$$[\mathbf{1}\cdot H\cdot A]^+ + B \rightarrow [\mathbf{1}\cdot H\cdot B]^+ + A \qquad (1)$$

The rate constants k' for the reaction defined in Equation (1) were obtained from the slopes of the pseudo-first-order rate plots ($\ln(I/I_0)$ versus t), where I is the abundance of complex $[\mathbf{1}\cdot H\cdot A]^+$ at the delay time t and I_0 is the sum of the abundances of $[\mathbf{1}\cdot H\cdot A]^+$ and $[\mathbf{1}\cdot H\cdot B]^+$. Irrespective of the configurations of A and B, linear rate plots are invariably observed with all $[\mathbf{1}\cdot H\cdot A]^+$ complexes except those with **1c**$_L$, Tyr; **1a**$_L$, dopa; and **1c**$_L$, dopa (see Figure 2 and Supporting Information).

The bimodal kinetics shown by these latter systems reveal the presence of several stable isomeric $[\mathbf{1}\cdot H\cdot A]^+$ structures. Above a certain reaction time, for example 6 s for $[(\mathbf{1c_L})\cdot H\cdot$(L-Tyr)$]^+$ and 12 s for $[(\mathbf{1c_L})\cdot H\cdot$(L-dopa)$]^+$ (Figure 2), the bimodal curves become linear (correlation coefficient $r^2 = 0.990$ and 0.976, respectively) which indicates that, at that delay time, only the less-reactive isomer $[\mathbf{1}\cdot H\cdot A]^+_{slow}$ is present. The time dependence of the more-reactive fraction $[\mathbf{1}\cdot H\cdot A]^+_{fast}$ can be inferred from the overall $[\mathbf{1}\cdot H\cdot A]^+$ decay after subtracting the first-order decay of the $[\mathbf{1}\cdot H\cdot A]^+_{slow}$ fraction. The good linearity of the resulting curve ($r^2 = 0.998$ and 0.991, respectively) suggests that only a single isomer is present in the more reactive $[\mathbf{1}\cdot H\cdot A]^+_{fast}$ fraction. Its y intercept, as well as that of the linear $[\mathbf{1}\cdot H\cdot A]^+_{fast}$ decay curve, provides an estimate of the relative distribution of $[\mathbf{1}\cdot H\cdot A]^+_{fast}$ and $[\mathbf{1}\cdot H\cdot A]^+_{slow}$, respectively (Table 1).

Table 1: Percent distribution of isomeric $[\mathbf{1}\cdot H\cdot A]^+$ structures.

Host (**1**)	Guest (A)	$[\mathbf{1}\cdot H\cdot A]^+_{fast}$	$[\mathbf{1}\cdot H\cdot A]^+_{slow}$
1a$_L$	D-dopa	20 ± 4	80 ± 4
	L-dopa	19 ± 3	81 ± 3
1c$_L$	D-Tyr	42 ± 3	58 ± 3
	L-Tyr	44 ± 2	56 ± 2
1c$_L$	D-dopa	48 ± 2	52 ± 2
	L-dopa	39 ± 3	61 ± 3

The second-order rate constants k, calculated from the corresponding $k'/[B]$ ratios, are listed in Table 2. Their values, compared with the relevant collision rate constants (k_{coll}),[10] provide a measure of the efficiency of the reaction (eff = k/k_{coll}, figures in parentheses in Table 2). The enantioselectivity factor ρ is defined as the ratio of the k value for the reaction of a given base B with the $[\mathbf{1}\cdot H\cdot A_D]^+$ complex and that for the same reaction with the $[\mathbf{1}\cdot H\cdot A_L]^+$ complex. The enantioselectivity factor ξ is defined as the ratio of the k value for the reaction of a given $[\mathbf{1}\cdot H\cdot A]^+$ complex with (*R*)-(−)-2-butylamine and that for the same reaction with (*S*)-(+)-2-butylamine. The $\rho < 1$ terms of Table 2 indicate that the $[\mathbf{1}\cdot H\cdot A_L]^+$ complex is more reactive than its $[\mathbf{1}\cdot H\cdot A_D)]^+$ diastereomer toward the same base B. The reverse is true when $\rho > 1$. The $\xi > 1$ terms of Table 2 indicate that (*R*)-(−)-2-butylamine is more reactive than (*S*)-(+)-2-butylamine toward the same $[\mathbf{1}\cdot H\cdot A]^+$ complex. The reverse is true when $\xi < 1$.

Comparative analysis of the kinetic data reported in Tables 1 and 2 shows the strict relationship between the structural features of the selected stereoisomeric hosts and their kinetic enantioselectivity toward a given chiral guest. In a previous study,[9] a structure (denoted as *up*) was assigned to the $[(\mathbf{1a_L})\cdot H\cdot(dopa)]^+_{fast}$ isomer in which the guest is located on the hydrophobic aromatic rim of the host. Conversely, in the $[(\mathbf{1a_L})\cdot H\cdot(dopa)]^+_{slow}$ structure (denoted as *down*), the guest is

Table 2: Exchange rate constants ($k \times 10^{-10}$ cm^3 molecule^{-1} s^{-1}).

Host (**1**)	Guest (A)	(*R*)-(−)-$C_4H_9NH_2$ *k*	eff	(*S*)-(+)-$C_4H_9NH_2$ *k*	eff	ξ
1a$_L$	D-Phe	3.60 ± 0.03	(0.32)	3.56 ± 0.04	(0.32)	1.01 ± 0.02
	L-Phe	2.20 ± 0.03	(0.20)	2.28 ± 0.04	(0.20)	0.96 ± 0.03
		ρ = 1.64 ± 0.03		1.56 ± 0.05		
	D-Tyr	0.86 ± 0.02	(0.08)	1.42 ± 0.02	(0.13)	0.61 ± 0.02
	L-Tyr	1.07 ± 0.02	(0.10)	1.36 ± 0.02	(0.13)	0.79 ± 0.02
		ρ = 0.80 ± 0.04		1.04 ± 0.03		
	D-dopa$_{fast}$	2.28 ± 0.06	(0.20)	1.26 ± 0.05	(0.11)	1.81 ± 0.12
	L-dopa$_{fast}$	3.00 ± 0.09	(0.27)	1.82 ± 0.20	(0.16)	1.65 ± 0.24
		ρ = 0.76 ± 0.04		0.69 ± 0.11		
	D-dopa$_{slow}$	$0.07_3 \pm 0.00_8$	(0.00_6)	$0.06_4 \pm 0.00_8$	(0.00_6)	1.14 ± 0.28
	L-dopa$_{slow}$	$0.10_0 \pm 0.00_8$	(0.00_9)	$0.07_9 \pm 0.00_9$	(0.00_7)	1.27 ± 0.25
		ρ = 0.73 ± 0.13		0.81 ± 0.19		
1b$_L$	D-Phe	4.06 ± 0.09	(0.36)	5.15 ± 0.06	(0.46)	0.79 ± 0.02
	L-Phe	3.78 ± 0.07	(0.34)	4.93 ± 0.06	(0.44)	0.77 ± 0.02
		ρ = 1.07 ± 0.05		1.04 ± 0.03		
	D-Tyr	2.29 ± 0.04	(0.21)	2.93 ± 0.03	(0.26)	0.78 ± 0.02
	L-Tyr	3.06 ± 0.06	(0.27)	3.81 ± 0.06	(0.34)	0.80 ± 0.03
		ρ = 0.75 ± 0.03		0.77 ± 0.02		
	D-dopa	1.57 ± 0.06	(0.14)	1.91 ± 0.06	(0.17)	0.82 ± 0.02
	L-dopa	1.47 ± 0.05	(0.13)	1.55 ± 0.05	(0.14)	0.95 ± 0.03
		ρ = 1.07 ± 0.07		1.23 ± 0.08		
1c$_L$	D-Phe	3.67 ± 0.04	(0.33)	3.61 ± 0.04	(0.32)	1.02 ± 0.02
	L-Phe	3.20 ± 0.05	(0.29)	3.25 ± 0.04	(0.29)	0.98 ± 0.04
		ρ = 1.15 ± 0.03		1.11 ± 0.03		
	D-Tyr$_{fast}$	3.39 ± 0.08	(0.30)	3.95 ± 0.11	(0.35)	0.86 ± 0.04
	L-Tyr$_{fast}$	3.24 ± 0.06	(0.29)	3.00 ± 0.13	(0.27)	1.08 ± 0.07
		ρ = 1.05 ± 0.04		1.32 ± 0.09		
	D-Tyr$_{slow}$	0.90 ± 0.03	(0.08)	0.97 ± 0.04	(0.09)	0.93 ± 0.06
	L-Tyr$_{slow}$	0.58 ± 0.03	(0.05)	0.61 ± 0.03	(0.06)	0.95 ± 0.09
		ρ = 1.55 ± 0.14		1.59 ± 0.13		
	D-dopa$_{fast}$	1.27 ± 0.03	(0.11)	0.87 ± 0.10	(0.08)	1.45 ± 0.23
	L-dopa$_{fast}$	0.47 ± 0.04	(0.04)	1.12 ± 0.10	(0.10)	0.42 ± 0.08
		ρ = 2.68 ± 0.30		0.78 ± 0.09		
	D-dopa$_{slow}$	$0.09_4 \pm 0.00_6$	(0.00_8)	$0.09_5 \pm 0.03_4$	(0.00_9)	0.99 ± 0.64
	L-dopa$_{slow}$	$0.04_1 \pm 0.00_5$	(0.00_4)	$0.04_6 \pm 0.00_8$	(0.00_4)	0.86 ± 0.35
		ρ = 2.30 ± 0.44		2.08 ± 1.33		

located at the hydrophilic rim of the host among the four chiral R pendant groups (Figure 1). The relative abundance of these isomeric structures (20 ± 4 versus 80 ± 4 %; Table 1) qualitatively conforms to their computed stability difference (20 kJ mol^{-1}).[9] The loss of dopa from the *up* structure of $[(\mathbf{1a_L})\cdot H\cdot(dopa)]^+_{fast}$ is promoted by the uptake of base B into the chiral hydrophilic rim of the host. This accounts for the high ξ values (1.81 ± 0.12 (D-dopa); 1.65 ± 0.24 (L-dopa)) in Table 2. A similar uptake is prevented in the *down* structure of $[(\mathbf{1a_L})\cdot H\cdot(dopa)]^+_{slow}$ by the presence of the guest in the hydrophilic cavity of the host. In this case, the amine B can only interact from outside the chiral cavity of the host, which can then exert only in part its asymmetry toward it (ξ = 1.14 ± 0.28 (D-dopa); 1.27 ± 0.25 (L-dopa); Table 2).

Similarly, the comparatively more level distribution of the isomeric $[(\mathbf{1c_L})\cdot H\cdot(dopa)]^+_{fast}$ and $[(\mathbf{1c_L})\cdot H\cdot(dopa)]^+_{slow}$ structures (48 ± 2 versus 52 ± 2 % (D-dopa); 39 ± 3 versus 61 ± 3 % (L-dopa); Table 1) indicates that their stability difference is somewhat reduced by the orientation of the chiral hydrophilic R pendant groups, not only along the *down*-like cavity of the host but also near its *up*-like region. This effect is also mirrored by the reduced difference in reaction rates of $[(\mathbf{1c_L})\cdot H\cdot(dopa)]^+_{fast}$ and $[(\mathbf{1c_L})\cdot H\cdot(dopa)]^+_{slow}$ relative to that of the $[(\mathbf{1a_L})\cdot H\cdot(dopa)]^+_{fast}$/$[(\mathbf{1a_L})\cdot H\cdot(dopa)]^+_{slow}$ pair (Table 2). The size and physical properties of the *up*-like and *down*-like regions of the chair stereoisomer $\mathbf{1c_L}$ are markedly different from those of the *up* and *down* regions of the flattened cone stereoisomer $\mathbf{1a_L}$. This may account for their opposite enantioselectivity toward dopa (ρ factors in Table 2). The diverse orientation of the incoming base B toward $[\mathbf{1}\cdot H\cdot(dopa)]^+$ ($\mathbf{1} = \mathbf{1a_L}, \mathbf{1c_L}$) may play a role as well, as suggested by the appreciable differences in the corresponding ξ terms (Table 2).

The apparently linear rate plots associated with the attack by base B on the diastereomeric $[(\mathbf{1b_L})\cdot H\cdot(dopa)]^+$ complexes can be correlated not only with the occurrence of a single complex structure, but also with the occurrence of different structures having comparable reactivity toward base B. Although no clear-cut evidence is presently available,[11] the reaction patterns shown by the ($[\mathbf{1}\cdot H\cdot(dopa)]^+$ (W = $\mathbf{1a_L}$; $\mathbf{1c_L}$) stereoisomers lend support to the latter hypothesis. This view conforms well with the ρ and ξ enantioselectivity values of the $[(\mathbf{1b_L})\cdot H\cdot(dopa)]^+$ complexes, which are in the middle of those of their $[\mathbf{1}\cdot H\cdot(dopa)]^+$ ($\mathbf{1} = \mathbf{1a_L}$, $\mathbf{1c_L}$) analogues (Table 2).

The general enantioselectivity picture shown by the $[\mathbf{1}\cdot H\cdot(dopa)]^+$ complexes finds some confirmation in their $[\mathbf{1}\cdot H\cdot(Tyr)]^+$ analogues. Although here the unequivocal assignment of two stable isomeric structures is limited only to the $[(\mathbf{1c_L})\cdot H\cdot(Tyr)]^+$ complex (Table 1), nevertheless the same ρ value trend is observed for both the $[\mathbf{1}\cdot H\cdot(Tyr)]^+$ and $[\mathbf{1}\cdot H\cdot(dopa)]^+$ series, which increases in the order: $\mathbf{1a_L} \leq \mathbf{1b_L} < \mathbf{1c_L}$ (Table 2). However, the complete absence of phenolic OH groups in Phe has a remarkable effect on the enantioselectivity of the reaction between base B and the corresponding $[\mathbf{1}\cdot H\cdot(Phe)]^+$ complexes. In contrast to their $[\mathbf{1}\cdot H\cdot(Tyr)]^+$ analogues, the $[\mathbf{1}\cdot H\cdot(Phe)]^+$ complexes invariably exhibit $\rho > 1$ values which increase in the reverse order: $\mathbf{1c_L} \sim \mathbf{1b_L} < \mathbf{1a_L}$. This selectivity picture finds some analogies with that observed in the gas-phase reaction of base B with

diastereomeric $[(\mathbf{1a_L})\cdot H\cdot A]^+$ (A = alanine (Ala) and serine (Ser)) complexes.[8,9] Indeed, $\rho > 1$ values have been measured for $[(\mathbf{1a_L})\cdot H\cdot(Ala)]^+$, whereas the $[(\mathbf{1a_L})\cdot H\cdot(Ser)]^+$ analogues invariably display $\rho < 1$ values. This opposite enantioselectivity is attributed to the different structures of $[(\mathbf{1a_L})\cdot H\cdot(Ala)]^+$ and $[(\mathbf{1a_L})\cdot H\cdot(Ser)]^+$, the first having the Ala guest located outside the host cavity in proximity to two adjacent pendant groups, and the latter having the Ser guest preferentially located inside the host cavity among the four pendant groups (the *down* structure).[9]

In conclusion, chiral recognition of the selected aromatic amino acids markedly depends on the structural features of the tetrakis(L-valinamido)[4]resorcinarene receptor, and mainly on the spatial orientation of its chiral R pendant groups. The flattened cone structure $\mathbf{1a_L}$ is characterized by a hydrophobic achiral (*up*) and a hydrophilic chiral (*down*) region. Dopa and Tyr, with OH functionalities on their aromatic ring, are preferentially hosted in the *down* region. Base-induced removal of their L enantiomers is faster than that of the D forms. The reverse is true for Phe where OH phenolic groups are absent. Two adjacent pendant groups lean outward from both the *up*-like and *down*-like cavities of $\mathbf{1c_L}$, and the other two lean over its *down*-like region. Both $\mathbf{1c_L}$ cavities seem capable of hosting the dopa and Tyr guests. In this case, base-induced removal of their L enantiomers is slower than that of the D enantiomers. Only one pendant group leans over the *up*-like structure of the 1,2-alternate stereoisomer $\mathbf{1b_L}$. The others form a sort of chiral *down* niche, which may accommodate better the selected amino acid guests. This may explain why the $[(\mathbf{1b_L})\cdot H\cdot A]^+$ complexes apparently exhibit only a single structural regioisomer, and why the base-induced removal of their amino acid guest displays the lowest measured enantioselectivity as regards both the configuration of the leaving guest and that of the incoming base.

Experimental Section

Optically pure $\mathbf{1a_L}$, $\mathbf{1b_L}$, and $\mathbf{1c_L}$ were coproduced from the $BF_3{\cdot}Et_2O$-catalyzed cyclization of the L enantiomer of (*E*)-*N*-[1-carboxyethyl)-2-methylpropyl]-2,4-dimethoxycinnamamide and isolated according to established procedures.[7] The D and L enantiomers of the amino acids (A) were obtained from Aldrich Co. and used without further purification. The same source provided the (*R*)-(−) (B_R) and (*S*)-(+) (B_S) enantiomers of 2-butylamine, which were purified in the vacuum manifold with several freeze–thaw cycles.

The experiments were performed at room temperature in an APEX 47e FT-ICR mass spectrometer equipped with an ESI source (Bruker Spectrospin) and a resonance cell ("infinity cell") situated between the poles of a superconducting magnet (4.7 T). Stock solutions of **1** (1×10^{-5} M) in 1:3 H_2O/CH_3OH, which contained a fivefold excess of the appropriate amino acid A, were electrosprayed through a heated capillary (130 °C) into the external source of the FT-ICR mass spectrometer. The resulting ions were transferred into the resonance cell by a system of potentials and lenses and thermalized by collisions with methane pulsed into the cell through a magnetic valve.[12] Abundant signals, which corresponded to the natural isotopomers of the proton-bound complex $[\mathbf{1}\cdot H\cdot A]^+$, were monitored and isolated by broad-band ejection of the accompanying ions. The $[\mathbf{1}\cdot H\cdot A]^+$ family was then allowed to react with the chiral amine B present in the cell at a fixed pressure of 4×10^{-8} to 3×10^{-7} mbar. Accurate measurement of the amine B pressure in the resonance cell necessitated the use of an ion gauge whose sensitivity was dependent on the nature of the chemical species. The correction of the ionization gauge reading was achieved by first determining the rate constant of the reaction between the $CH_4^{\cdot+}$ radical cation and CH_4 in the FT-ICR instrument at a given nominal methane pressure, and then comparing the result obtained with the average value of the rate constants reported for this process (1.13×10^{-9} cm^3 molecule^{-1} s^{-1}).[13] Subsequently, the correction factor needed for amine B was estimated by using the method based on an indicated linear dependence of the response of the ionization gauge with the polarizability of the base in question.[14]

Received: May 14, 2004

Keywords: enantioselectivity · enzyme models · host–guest systems · kinetics · macrocycles

[1] F. Diederich, *Angew. Chem.* **1988**, *100*, 372; *Angew. Chem. Int. Ed. Engl.* **1988**, *27*, 362.
[2] J.-M. Lehn, *Angew. Chem.* **1988**, *100*, 91; *Angew. Chem. Int. Ed. Engl.* **1988**, *27*, 89.
[3] D. Cram, *Angew. Chem.* **1988**, *100*, 1041; *Angew. Chem. Int. Ed. Engl.* **1988**, *27*, 1009.
[4] K. S. Jeong, J. Rebek, Jr., *J. Am. Chem. Soc.* **1988**, *110*, 3327, and references therein.
[5] N. Pant, A. D. Hamilton, *J. Am. Chem. Soc.* **1988**, *110*, 2002.
[6] For recent reviews on gas-phase enantioselectivity, see: a) M. Speranza, *Adv. Phys. Org. Chem.* **2004**, *39*, 147; b) M. Speranza, *Int. J. Mass Spectrom.* **2004**, *232*, 277.
[7] B. Botta, G. Delle Monache, P. Salvatore, F. Gasparrini, C. Villani, M. Botta, F. Corelli, A. Tafi, E. Gacs-Baitz, A. Santini, C. Carvalho, D. Misiti, *J. Org. Chem.* **1997**, *62*, 932.
[8] B. Botta, M. Botta, A. Filippi, A. Tafi, G. Delle Monache, M. Speranza, *J. Am. Chem. Soc.* **2002**, *124*, 7658.
[9] B. Botta, A. Tafi, M. Botta, G. Delle Monache, A. Filippi, M. Speranza, *Chem. Eur. J.* **2004**, *10*, 4126.
[10] T. Su, *J. Chem. Phys.* **1988**, *88*, 4102–4103, 5355.
[11] Careful inspection of Figures in the Supporting Information does not exclude the possibility of bimodal reaction kinetics between base B and the diastereomeric $[(\mathbf{1b_L})\cdot H\cdot(dopa)]^+$ complexes.
[12] Observation of the same time dependence of $[\mathbf{1}\cdot H\cdot A]^+$ when unquenched or collisionally quenched by methane in the FT-ICR cell indicates that the $[\mathbf{1}\cdot H\cdot A]^+$ complexes are translationally and vibrationally thermal when reacting with base B.
[13] Y. Ikezoe, S. Matsuoka, M. Takebe, A. A. Viggiano, *Gas-Phase Ion–Molecule Reaction Rate Constants Through 1986*, Maruzen Company, Tokyo, **1987**.
[14] J. E. Bartmess, R. M. Georgiadis, *Vacuum* **1983**, *33*, 149.

